Trans Indian Inst Met (2017) 70(10):2485–2496
DOI 10.1007/s12666-017-1120-z

REVIEW PAPER

First Report on the Deformation Mechanism Mapping of First and Second Generation Ni-Based Single Crystal Super Alloys

M. Kamaraj[1] · **V. M. Radhakrishnan**[1]

Received: 13 October 2016 / Accepted: 17 March 2017 / Published online: 8 April 2017

Abstract Nickel based single crystal super alloys are widely used as aircraft engine blades and are still in the process of development to improve the high temperature capabilities. The typical microstructure of these alloys consists of gamma phase as the matrix strengthened by the gamma prime precipitates. In recent times, addition of refractory metals like Re are tried to improve the creep strength. The first generation of these alloys does not contain any such additions. The second generation of the alloys contains around 3–6% Re. These additions and modifications have been found to improve the temperature capability of the CMSX, though there are limitations in their addition. In this article the microstructural developments, the metallurgical and high temperature behavior of the first and second generation NiSX family subjected to stress annealing, are discussed from engineering point of view. Based on experimental findings reported in literature, deformation maps illustrating the different mechanisms over a wide range of temperature and stress levels for the first and second generation alloys are presented.

Keywords NiSX · Gamma-prime precipitate · Rafting · Particle shearing · Deformation · Mapping

1 Introduction

Microstructure of the Ni-base super alloy single crystals has cubical gamma prime precipitates, $Ni_3(Al, Ti)$, aligned in vertical and horizontal columns and rows in the gamma matrix which form vertical and horizontal channels. The volume fraction of gamma prime precipitates may range from 50 to 70% and the rest of the gamma matrix is arranged as channels separating the gamma prime precipitates. The size of the gamma prime precipitates may range from 200 to 500 nm. The absence of grain boundary strengthening elements in NiSX allows heat treatment of the alloy at high temperature. This will help to refine the gamma prime precipitates which will increase the high temperature strength.

During unstressed aging, the gamma prime particles typically undergo transition from spherical to cubic and then to irregular morphologies. A typical micrograph of a properly heat treated NiSX with gamma prime precipitates in the gamma matrix is shown in Fig. 1 [11].

Heat treatment is a very important step to obtain the alloy with best properties. Proper heat treatment including correct sequence in aging time and temperature, must be followed to obtain well refined cohesive gamma prime precipitates. Underaging will result in spherical type precipitates and, overaging will result in irregular wavy lamellar structure, both will weaken the material. So aging treatment must be properly controlled to result in coherent cubical gamma prime precipitates in gamma matrix at the end of the treatment.

2 Microstructural Details of First and Second Generation NiSX Alloys

In high technology engineering applications, the NiSX alloys will be subjected to a wide range of stress and temperature, typically stress from 50 to 1000 MPa and temperature from 500 to 1200 °C. So investigations and characterization of the deformation processes in these regions have been carried out by a number of researchers in the last three decades. In these ranges of stress and

✉ M. Kamaraj
kamaraj@iitm.ac.in

[1] Department of Metallurgical and Materials Engineering, Indian Institute of Technology Madras, Chennai, Tamil Nadu 600036, India

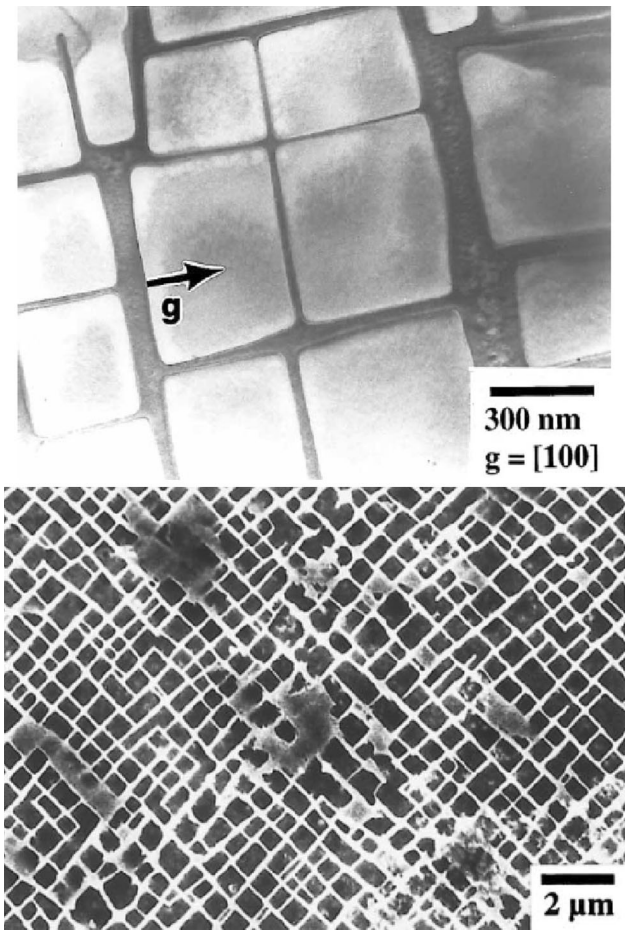

Fig. 1 Micrograph of heat treated NiSX

temperature under isothermal condition, there are varieties of microstructural changes that take place in the alloys contributing to the deformation processes. They can be, in general, summarized as follows.

1. Dislocations generation, multiplication and glide
2. Coarsening of gamma prime precipitates
3. Formation of gamma prime rafts
4. Widening of gamma matrix channels
5. Dislocation glide and climb
6. Cutting of gamma prime particles by dislocation
7. Shearing of gamma prime rafts
8. Formation of pair of dislocations and super dislocations
9. Formation of Rhenium clusters in gamma matrix in second generation alloy
10. Sluggish diffusion and nil coarsening or raft formation
11. TCP phase formation

All these and other associated microstructural changes during stress annealing in first and second generation NiSX alloys are discussed and the overall pictures of deformation mechanisms are presented as maps.

3 Microstructural Changes and Deformation Mechanism

3.1 Gamma Prime Coarsening and Raft Formation Mechanism

Growth of gamma prime particles and subsequent raft formation are due to the plastic strain induced by the applied stress. In this strain-induced rafting process, the presence of chemical gradients between the vertical and horizontal gamma matrix channels provide the driving force for rafting. These gradients are attributed to the segregation of gamma-forming elements at the interfacial dislocations which are formed preferentially within the horizontal gamma channels during the early stage of deformation. Due to these gradients, rafting is assumed to take place by cross flow of gamma forming elements to the horizontal gamma-channel and gamma prime-forming elements to the vertical gamma channels, giving rise to the rafted structure. A typical coarsening mechanism is schematically shown in Fig. 2.

Due to these rearrangement of elements, raft formation takes place and a typical micrograph of raft formation is shown in Fig. 3 [10].

3.2 Factors Affecting Rafting [1, 8, 16, 17, 19, 33]

3.2.1 Orientation of Applied Stress [4, 20–22, 35, 36]

Misfit between gamma and gamma prime phases, temperature and applied stress, externally induced plastic strain—all these factors govern the formation and growth, the kinetics and morphology of rafts. Analyzing the rafting process in creep, Pollock and Argon [24, 25] have concluded that directional gamma prime precipitate

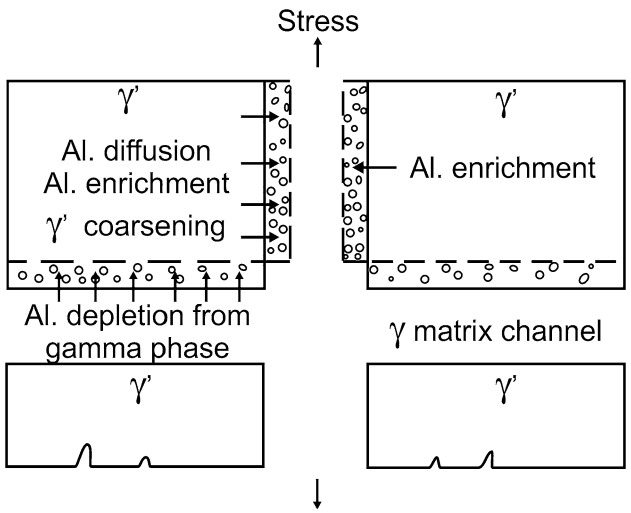

Fig. 2 Schematic representation of gamma prime coarsening

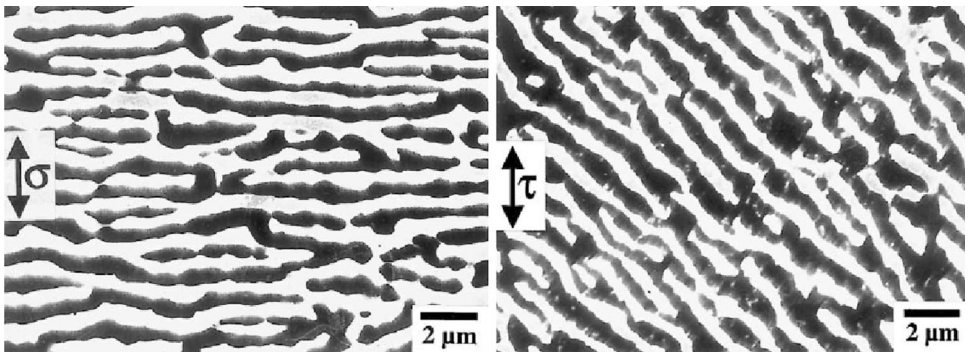

Fig. 3 Micrograph of raft formation

coalescence is accomplished by preferential local dissolution of the gamma prime particles and diffusional flow of the alloying elements to adjacent matrix channels. A detailed analysis of raft formation and the factors affecting rafting are well documented by Tien and Cobley [33].

Two types of directional rafting behaviour in (001) oriented Ni based single crystals have been identified. Type N (normal to stress direction)—these are elongated precipitates or rafts grown transverse to the direction of the externally applied stress. Type P (parallel to stress direction)—these are rafts developed parallel to the direction of the externally applied stress [4].

3.2.2 *Role of Misfit*

Rafting is mainly controlled by lattice misfit. The difference in the lattice parameters of gamma and gamma prime leads to misfit, defined as

$$\text{MF} = 2\,(\text{Lp gamma prime} - \text{Lp gamma})/ (\text{Lp gamma prime} + \text{Lp gamma})$$

In most super alloys (SRR 99, CMSX-2, CNSX-4, CMSX-6), the lattice misfit at room temperature is small and negative (approx. $= -.003$ to -005).

As a result of the negative misfit, hydrostatic coherency stresses (both tensile and compressive) are introduced around the gamma prime precipitate faces. When an external stress is applied, the stress condition will change, and a driving force will develop in the channels leading to coarsening of the gamma prime precipitates and subsequent rafting particles [6, 18, 19].

Type N rafting is observed when misfit is negative and stress is in tension and also when misfit is positive and stress is in compression. Type P rafting is observed when misfit is positive and stress in tension and also misfit is negative and the stress in compression.

Rafting process is often fairly complete by the end of the primary creep transient, because directional coarsening is influenced by the internal misfit stresses and large creep deformation in the later stage will relieve these misfit stresses and will be replaced by creep flow. Generally, the rate of rafting increases with misfit.

3.2.3 *Growth of Rafts and Change in Channel Width [20–22, 33]*

A large volume of research articles has been published on the raft formation and growth, the factors influencing the raft size and orientation, the internal and external stresses, alloy chemistry, the dislocation structure and the channel width etc., in the last two decades. The effects of heat treatment, temperature, the time of exposure of the crystal to high temperature and stress have also been well documented.

Volume fraction of the gamma prime will also determine the nature and process of coarsening. The matrix in low volume fraction alloys will not be so highly stressed by the presence of misfit precipitates and further coalescence will be more difficult with widely dispersed precipitates. Internal misfit stresses as well as plastic flow processes are important to the development and growth of rafted precipitates.

The width of the gamma matrix channel will increase as the rafting continues. The gamma channel widening is controlled by a multi atom diffusion process through the channels. In case of multi-axial loading, the normal stress components perpendicular to the gamma/gamma prime interface are important.

Widening of gamma channel follows a parabolic rate law. This widening may act as a microstructural softening as it will allow more dislocations to glide through.

After stable raft formation, the channel width increment will lead to coarsening of the rafts and increased deformation. Growth of raft and change in channel width with exposure time are shown in the micrographs given in Fig. 4 [21].

3.2.4 *Role of Raft in Deformation*

Finer gamma prime plates will provide more interface per unit volume. The refined gamma prime particles size and

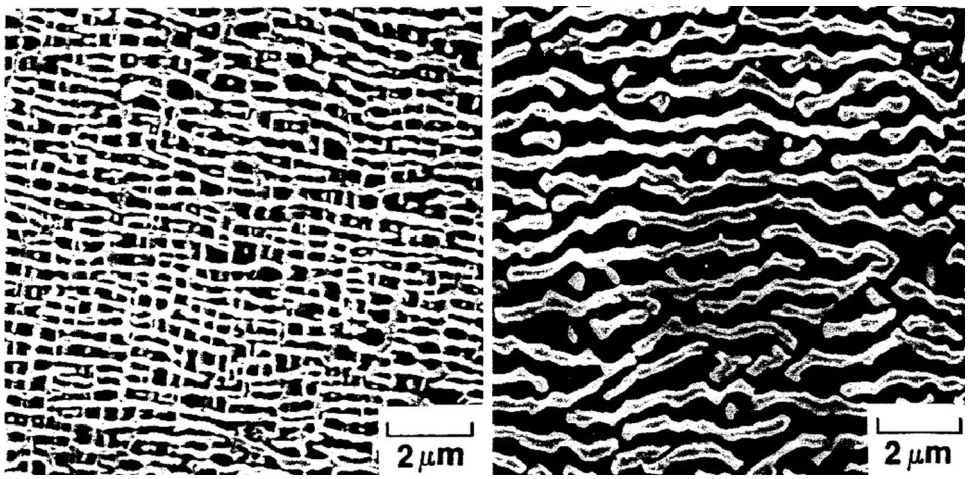

Fig. 4 Micrograph of growth of raft and change in channel width with time

thus, the lamellar thickness will reduce the deformation rate. However, when the plate thickness increases with increasing time, the density of gamma–gamma prime interface will decrease, resulting in increased deformation rate.

At intermediate temperatures and stresses, dislocation activity is restricted in the gamma matrix and at high stresses in the temperature range of 750–850 °C gamma prime shearing and activation of (112) {111} slip are commonly observed.

In low temperature high stress region (LTHS), rafting increases the creep deformation, reduces the creep resistance because the dislocations climb the gamma prime phase and glide. In high temperature low stress region (HTLS), rafting suppresses creep deformation and improves creep performance because dislocations have to shear the gamma prime phase or raft. Thus, creep mechanism changes from dislocation climb around the gamma prime precipitates in LTHS to the dislocation cutting through the gamma prime rafts in HTLS.

Rafting has been considered by some investigators as a hardening process which will enhance the creep resistance of SX alloys in (001) orientation. When the lamellar structure is formed perpendicular to the stress axis (with negative misfit), the movement of dislocations by climb over the gamma prime particles will be difficult. More diffusional processes and shearing of gamma prime should occur for creep deformation. Thus, the resistance to deformation will increase. Other investigators have opined that directional coarsening will decrease high temperature mechanical properties.

3.3 Dislocation Glide and Climb, Cutting and Shearing of Raft

Contributions to deformation by dislocations multiplication, gliding, cutting and shearing, formation of super dislocations APB etc., depend on state of stress and temperature. In the following, the deformation mechanisms due to dislocations are discussed in the ascending line of stress and temperature.

Generally, deformation characteristics are controlled by the processes, namely (1) the increase of dislocation density in the gamma channels (dislocation glide and dislocation climb) which controls primary creep (2) pair wise cutting of two dislocations from a gamma channel into the gamma prime followed by their annihilation and (3) the widening of gamma channels associated with rafting in later stages of creep which can result in steady increase in deformation rate [11].

At low deformation rates, strength depends on the shear of the gamma prime particles. At moderate and high strain rates, slip occurs by the coupled motion of pairs of dislocations and the resistance to the motion of these pairs occurs at the gamma/gamma prime interfaces. Close spacings between the particles offer high resistance and so the pair of dislocations must penetrate and shear these interfaces to cause deformation.

Interfacial dislocations accumulated at gamma/gamma prime interfaces play important role in deformation. Dislocations gliding in the gamma channels will draw out the interface dislocations which can move by glide—climb motion along the horizontal gamma/gamma prime interfaces under the combined action of the applied stress. This thermally activated glide-climb motion is the rate controlling process. Dislocations reach the edge of the plates and glide across the vertical channel as shown schematically in Fig. 5.

When the internal forward stresses in the gamma prime plates reach a critical value, the dislocations can cut the gamma prime faces. The build-up of internal stresses will depend on stress and temperature. If the critical value is not reached, the dislocations will circumvent the gamma prime plates by glide and climb process. If the dislocation-by-pass

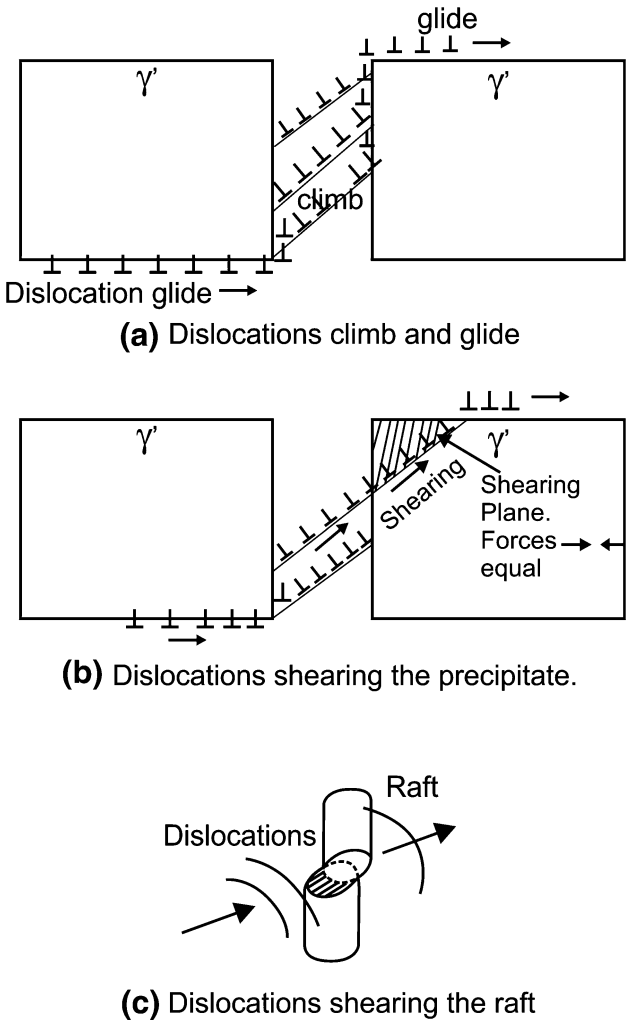

Fig. 5 Schematic view of dislocation glide, climb and shear of raft

is suppressed by the rafted morphology, then gamma prime shearing will come into effect leading to a recovery process.

Effect of shearing: large amount of precipitate shearing will lead to super lattice stacking faults (SSF) (observed in CMSX-4 alloy at 750 °C/800 MPa). Matrix dislocations dissociate into (1) a super Shockley partial which shears the precipitate leaving a super lattice intrinsic stacking fault (SISF) and (2) another partial which remains at the interface boundary (APB). The dominant mode of gamma prime shear is through generation of SISF. At high temperatures (1000 °C), precipitate shear occurs exclusively by APB mechanism.

4 Developments in Ni Based SX

4.1 Generation-Wise Developments

The Ni SX alloys were developed as first and second generations, each containing high Cr and no Re or addition of Re with reduced Chromium. Typical alloys in their trade names are given below.

First generation Ni SX without Re and with high Cr (8–14%) PWA 1480, Rene N4, SRR 99, RR 2000, AM1, AM3, CMSX-2, CMSX-3, CMSX-6, CMSX-11B, CMSX-11C.

Second generation Ni SX with Re 0.5–3% and Cr (5–8%) CMSX-4, PWA 1484, SC 180, Rene N5, MC 2.

The NiSX alloys initially developed were of non-Rhenium containing type and generally gave around 20 °C more strength improvement relative to directionally solidified alloys. As the advantage of addition of Re became known, the second generation containing up to 3% Re came as a promising candidate material exhibiting about 30–35 °C improved strength. The second generation gained commercial significance. Further development with increased Re of about 6% and moderate (Al + Ti) and lower chromium and higher cobalt content is now being explored and experimented for higher thermal capacity.

4.2 First Generation of NiSX (Cannon-Muskegon Corp, CMSX Single Crystals) [3, 9, 20–22]

The single crystal Ni-base super alloys do not require the grain boundary strengtheners like C, B, Zr and Hf. However, elements like cobalt, tantalum and tungsten, apart from Al, Cr, Ti and Mo are added and they play important roles in influencing the properties like solvus, precipitate size and shape, volume fraction, lattice parameter and coarsening rate of gamma prime phase of these single crystals. The coarse gamma prime present in the as-cast micro structure of the single crystal must be completely dissolved and re-precipitated as fine dispersion. The large difference between the solidus and the gamma prime solvus will enable all alloys to be properly solution treated.

Effects of Co, Ta, and W to Ni base single crystals have been studied by Nathal and Ebert [20–22] with negative lattice misfit [$=2(ar' - ar)/(ar' + ar)$] equal to 0.003. Decrease in Co content from 10 to 0 pct has been found to increase the solvus of gamma prime. The solvus decreases when Ta is removed in the alloy, because Ta partitions strongly to the gamma prime phase. Substitution of W for Ta produces an intermediate reduction of the solvus as W partitions less strongly to gamma prime. High levels of elements which partition strongly to gamma prime, promote higher volume fractions of gamma prime and increase its stability. Tantalum is a strong gamma prime former and tungsten partitions less strongly to gamma prime. Cr, Co, and Mo partition preferentially to gamma phase whereas Al, Ti and Ta partition to gamma prime. The refractory metals like W and Ta have significant contribution to solid solution strengthening mechanisms.

The gamma prime lattice parameters appear to be nearly independent of Co content. When Co content is increased, only Co and Ni concentrations in gamma prime are changed as Co and Ni have very small differences in atomic size and, so the lattice parameter of gamma prime will not be very much affected. As Co level is increased from zero, a decrease in the magnitude of the lattice misfit is observed, the effect being mainly due to changes in the gamma lattice. However, it should be noted that the value of lattice misfit at room temperature can vary significantly at elevated temperature and tend to be more negative as the temperature is increased.

CMSX-2 Nominal composition by wt% Co = 4.5%, Cr = 8.5%, Mo = 0.65%, W = 8.0%, Al = 6.0%, Ti = 1.0%, Ta = 5.5%, Hf < 0.1%, Zr = 0.01%, C = 50ppm, Ni Balance.

Heat treatments which lead to aligned cuboidal precipitates of about 0.45 micron in size, considerably improve the creep strength of CMSX-2 in the temperature range of 800–1050 °C. Shearing of precipitates by {111} <112> slip is a general feature of deformation mechanism during primary creep of CMSX-2. In secondary creep, the shearing of precipitates by constricted dislocation pairs is also present. The lower creep rate for aligned cuboidal precipitates is due to higher stability of dislocation net work at the gamma–gamma prime interface. When perfect rafting forms at high temperatures (1000 °C/300–500 MPa), climb around gamma prime rafts becomes difficult and at higher stresses, these rafts are sheared by dislocation pairs.

CMSX-3 Nominal composition by wt% Co = 4.5%, Cr = 8.0%, Mo = 0.5%, W = 8.0%, Ti = 1.0%, Al = 5.5%, Ta = 6.0%, Hf = 0.1%, Ni balance

CMSX-3 subjected to creep at moderate temperature and stress levels (800 °C/550 MPa) shows an incubation period in virgin crystals, prior to the onset of primary creep. The incubation period is due to dislocations filling up the matrix channel which is initially free from creep dislocations. When the newly generated creep dislocations fill up the cross section of the matrix, the incubation period ends and the primary creep starts. In the primary creep period, creep rate decreases because the thermal misfit stresses between gamma and gamma prime phases are relieved by creep flow. Continued creep leads to a buildup of a three-dimensional nodal network of dislocations which fills the gamma matrix channels. Gamma prime particles are difficult to penetrate and dislocations move through the gamma matrix by forced Orowan bowing, causing resistance to creep.

4.3 Second Generation of Ni SX Alloys (with Re Addition Up to 3%) [7, 14–16, 27, 28, 32, 35]

Deformation and creep properties of Ni base single crystal superalloys with Re = 0.5%, Cr = 9%, Mo = 0.5%, W = 2.4%, Al = 11.5%, Nb = 1.2%, Ta = 3.0%, have been investigated by Masakazu Saito et al. [16] in the temperature range of 1040 °C under 137 MPa with orientation in the [010] direction. Diffusion of Al and rafting mechanism in low Re level (Re = 0.5%) have been studied in detail. After 2 h of creep test, Al concentration increases in the gamma prime phase areas near gamma/gamma prime inter face perpendicular to applied tensile stress and it decreases in the gamma prime phase area near the gamma/gamma prime interface parallel to the applied tensile stress. Chromium concentration is also affected in the interface. Tensile stress increases the elastic strain energy parallel to the stress and decreases the same perpendicular to the stress in the gamma prime phase near the gamma/gamma prime interface. New equilibrium conditions are thus obtained which causes swelling and shrinking of the gamma prime phase resulting in a tendency to raft formation normal to the applied tensile stress in HTLS region.

To optimize CMSX alloy creep properties, it is necessary to increase the total refractory metal concentration for both solid solution strengthening in the gamma matrix and order strengthening in gamma prime precipitates. Addition of refractory metals also alters the lattice mismatch between the coherent gamma prime precipitates and the gamma matrix and retards diffusional coarsening of gamma prime precipitates in lower temperature region <800 °C. However, the refractory metals have propensity to form topologically close packed (TCP) phases such as Sigma, Myu, and Laves in the temperature range of T = 800–900 °C.

CMSX-4 The nominal composition of CMSX-4 (wt%) can be given as Cr = 6.4%, Al = 5.7%, Ti = 1.0%, Mo = 0.6%, W = 6.3%, Ta = 6.5%, Co = 9.5%, Hf = 0.1%, Ni: balance, with Re around 3%.

CMSX-4 contains Rhenium (Re) which is added to most of the advanced generation SX alloys to reduce the rate of diffusion. However, Re being costly, addition of Re in Ni SX will increase the cost of the end product.

Role of Rhenium The effect of addition of Rhenium to Ni based alloy has been investigated in detail by Giamei and Anton [7] and Schneider et al. [27, 28].

(a) Addition of Re will reduce the rate of diffusion and retard the coarsening of the gamma prime phase at temperatures up to 800 °C.
(b) It also increases the strength of the matrix by the formation of small Re clusters = 1 nm in diameter.
(c) The presence of Re will hinder the development of raft in the lower regions of high temperature T < 800 °C. A typical case of Rhenium eliminating rafting of CMSX-4 at 800 °C and 640 MPa stress is shown in the micrograph in Fig. 6. The micrograph also shows the formation of rafts at 950 °C and 301 MPa stress [28]. Raft formation in Re containing

alloys has been observed above the temperature of 900 °C.

(d) Rhenium, like other refractory metals, increases the lattice parameter of gamma substantially. The negative misfit between gamma prime and gamma matrix is increased by the refractory metal resulting in improved creep life. Further, in Ni based single crystals with Re additions (6%), long stacking faults (SF) of several micron lengths are observed which take part in shearing of gamma matrix leading to lowering of creep rate [37].

(e) Addition of Re improves creep properties because Re is mainly distributed in gamma matrix phase to form atom clusters with short range ordering which will hinder the dislocation movement and decrease the diffusion rates of elements and gamma prime directional growth. Re atoms dissolved in gamma/gamma prime phases will also delay dislocation shearing into the gamma prime phase-the main mechanism of creep deformation [32, 34, 35].

Under HTHS creep condition (950 °C/350 MPa), CMSX-4 with Re = 3% in high volume fraction shows formation of deformation twins and super lattice stacking faults. The formation of high temperature twining is associated with the loading orientation in which SESF formation is expected. In the temperature region of 800–900 °C, Rhenium causes formation of TCP phases and also SRZ (secondary reaction zone) under protective coatings.

Tests conducted on CMSX-4 at 1100 °C clearly indicate the presence of particles rich in W, Re, and Mo, possibly produced and precipitated when the material passes through the temperature range of 800–900 °C. Figure 7 shows the precipitated TCP phases [27, 28].

Creep behaviour of a new Ni SX containing 4.5% Re has been analyzed by Sugui Tian et al. [30] in the temperature range of 760–800 °C at stress levels of 800–840 MPa. Coherent gamma prime precipitates in gamma matrix are observed with dislocation movement in the matrix as the main mechanism of deformation. Compared to non-Re containing Ni SX alloys, the alloy thus investigated shows better creep resistance and longer creep life. Super dislocations that form, decompose on (111) planes and form super Shockley partials and stacking faults. These will hinder dislocation movement and restrain cross slipping of dislocations, leading to alloy having better creep resistance at intermediate temperature.

Creep behaviour of Ni SX with Re = 4.2% in high temperature region of 1040–1100 °C and stress from 120 to 150 MPa, has been investigated by Sugui Tian et al. [31, 32]. They found that the creep rate follows a power function of stress with n = 4.7 and the activation energy Q = 483 kJ/mol. The dislocation climbing over the rafted gamma prime phase dominates the creep process at low stress of 120 MPa. In the later stages of creep, super dislocations shear into the rafted gamma prime phase. The main and secondary slipping dislocations are alternately activated to twist the gamma prime rafts up to the last stage of creep. In the temperature of 1040–1100 °C, the alloy with Re = 4.2%, show better creep resistance as compared to alloy with Re = 2%.

5 Deformation Mechanisms Demarcation and Mapping of First and Second Generation Alloys

5.1 Classification and Identification of Regions and Mapping of First Generation Alloys

5.1.1 Introduction

As the microstructural changes which are responsible for deformation in NiSX, are controlled by the applied stress and temperature, they can be broadly classified and

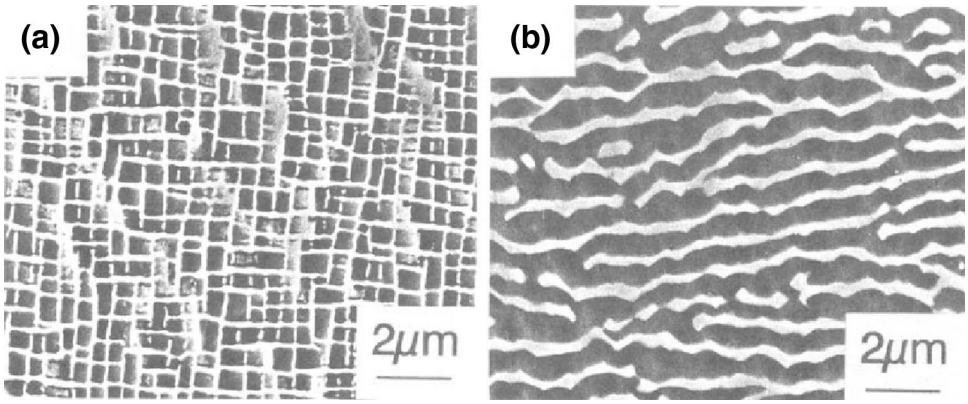

Fig. 6 Micrographs showing the suppression of raft formation in Re containing CMSX-4 **a** below 800 °C and **b** above 950 °C

Fig. 7 Micrograph of CMSX-4 at 1100 °C indicating TCP particles rich in W, Re, and Mo

identified on the stress-temperature coordinates and, can be in general represented by four regions as follows.

1. Low temperature/low stress (LTLS)
   (*dislocation build up in gamma channel, *dislocation multiplication in gamma channel, *dislocation glide, *gamma prime cubes, *precipitate growth, *raft formation, *low deformation rate)
2. Low temperature/high stress (LTHS)
   (*raft formation and growth, *channel widening, *dislocation glide and climb, *dislocation network formation)
3. High temperature/low stress (HTLS)
   (*raft formation and growth, *shearing mechanism, *pair of dislocation, *super dislocation formation, *turbine blade application region)
4. High temperature/high stress (HTHS)
   (*rapid widening of channel, *high deformation rate, *rafts breaking, *short creep life)

These four regions and the dominant mechanisms of deformation of first generation NiSX, stressed in [001] orientation, are indicated schematically in Fig. 8. Some mechanisms may cross the boundary and extend to other adjacent regions. However, the mapping will give the overall possible microstructural activities in NiSX alloys, well heat treated and aged to give coherent cuboidal gamma prime precipitates.

5.1.2 Microstructural Regions in First Generation Alloys [23]

1. Low temperature/low stress region (LTLS)
   (400–700 °C/100–500 MPa) [23]

When the temperature and stress levels are low, initial incubation time for creep to occur has been observed. During the period of incubation, dislocations are generated and multiplication occurs in the gamma channel. When the dislocations are being generated and when they multiply, the movement of the dislocations in the gamma channels will be relatively easy and creep strain can be high. The cuboidal precipitates consolidate as they grow. The multiplication of dislocations into a net work shape and the formation of precipitates and their growth will decelerate the movement of dislocations, thereby reducing the creep strain rate. In the higher side of this region of temperature and stress, raft formation will be favoured (N/P) depending on the orientation of the applied stress.

2. Low temperature/high stress region (LTHS)
   (400–700 °C/600–1000 MPa)

Investigations in this regime of LTHS have revealed that the well aligned cuboidal gamma prime precipitates in gamma matrix channel are formed and the gamma channels are narrow in the initial stages. Loops of dislocations enter the narrow gamma matrix channels where they have to overcome Orowan stress associated with the gamma channel width. The filling of gamma channels with dislocations governs the primary stage of creep. As the density of dislocations and their interaction increases due to filling of the channel width, their movement slowly gets restricted and creep strain rate starts decreasing. However, as the rafting of gamma prime starts and grows, the gamma matrix channel width "W" widens, giving more room for the dislocation movement, a phenomenon similar to softening process which tries to overcome the hardening process due to dislocation interaction, thus leading to a balance.

Investigations by Kamaraj [10–12] have shown that the width of the gamma channel is a distributed quantity and follows log normal distributions. The width "W" of the channel in the course of rafting follows a parabolic rate law, i.e. "W" = A $(t)^{0.5}$ suggesting that a multi atom diffusion through the channels governs their widening. The stress perpendicular to the gamma/gamma prime interfaces is also important in controlling channel width.

N or P rafting, slip in gamma matrix channel and increase in width of the channel are commonly observed in LTHS. Glide and climb of dislocations at the gamma/gamma prime interface appear to control the deformation.

3. High temperature/low stress region (HTLS)
   (750–1200 °C/50–400 MPa) [2, 23, 24, 26]

This region is encountered in practical gas turbine applications and the turbine blades face a temperature range of 800–1200 °C and a maximum stress of around 400 MPa. Large volumes of experimental investigations and structural analyses have been carried out by many researchers in HTLS.

In the region HTLS (long time creep) where high temperature replaces the role of high stress in the dislocation mechanism, the cuboidal gamma prime particles are

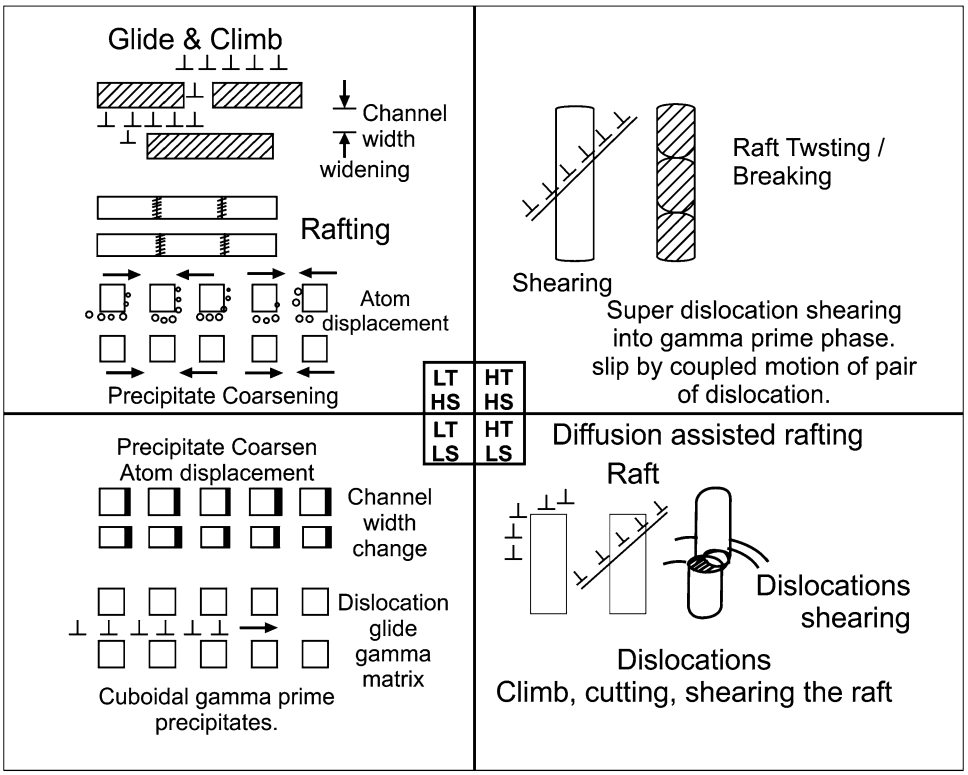

Fig. 8 Schematic representation of different mechanisms in the four regions of stress and temperature

transformed after a very small plastic strain (0.1%) to plate like gamma/gamma prime rafts. In low temperature side, the diffusional processes are slow and the cuboidal gamma prime particles are preserved. The dislocations move in the horizontal gamma matrix channel under small plastic yielding. This movement of dislocations will stop at the gamma/gamma prime interface. As the deformation continues, the dislocations will glide and climb in the vertical channel in-between the gamma prime particles or rafts and the deformation will continue.

The deformation mechanisms that are normally encountered in both LTHS (700–850 °C/600–800 MPa) and HTLS (900–1100 °C/100–300 MPa) overlap in many cases and can be summarized as follows.

1. Slip and multiplication of dislocations in discrete slip system of the gamma matrix.
2. Dynamic recovery of the dislocation structure. The dislocation loops spanning around the gamma prime particles move by the combination of slip and climb along the gamma/gamma prime interface and shrink towards the apices of the gamma prime particles.
3. Morphological changes of gamma prime precipitates by migration of gamma/gamma prime interfaces related with diffusion transport of elements compensating the differences in chemical composition of the gamma matrix and the gamma prime particles.
4. Cutting of the gamma prime particles. The dislocations generated in the gamma matrix penetrate the interface and slip through the gamma prime particles.
5. Coarsening of the rafted structure and rapid widening of the gamma channels.

Investigations have been carried out on CMSX-4, CMSX-6 at 1080 °C and stress = 50 MPa [10–12] to study the dislocation kinetics in the initial stages of high temperature deformation. Number of investigations on other NiSX alloys have also been carried out in this region to understand the microstructural mechanisms [5, 9, 28, 29, 37].

Cutting of the gamma prime phase by dislocations and the movement of super dislocations are widely studied. During high temperature/low stress creep, the creep rate increases as the temperature increases. Primary cuboidal gamma prime (size 400–450 nm) particles change shape to aid the growth of gamma prime raft. Dislocations cut or by pass the precipitates to cause creep deformation. At 700 °C dislocations move along the matrix channel and, gamma prime shearing by stacking fault and dislocation pair is also observed. Some times bypassing of gamma prime particles by dislocations also takes place.

As the temperature is increased at 1025 °C and shear stress = 85 MPa in CMSX6 crystal, investigations show that more than one slip system of the type <110> {110} are activated. During primary creep in HTLS region, initially

the channel dislocations do not cut the gamma prime particles. With increase in dislocation density work hardening takes place and this is followed by the cutting of gamma prime particles and dominates up to minimum creep rate of around 2% shear strain.

4. High temperature/high stress region (HTHS) (800–1100 °C/700–1000 MPa)

In this region, super dislocations form and diffusion plays important role in deformation. Gamma prime is cut by super dislocations which glide on a {111} plane, as observed in CMSX-2 crystals. The widening rate of the gamma channel will be higher and the gamma prime rafts that have formed may slowly crumble leading to higher deformation rate. This region of high temperature (>1000 °C) and stress (>500 MPa) is not normally encountered and hence experimental data are limited.

The deformation mechanism map of the first generation NiSX alloy is shown in Fig. 9. The contours of strain rates are also indicated in the figure. Though large volume of experimental data is available, for clarity sake, not all data points are shown in the map. In the LTLS region, creep deformation will be slow and so the strain rate will be low. In the HTHS region, creep rate will be rapid resulting in higher strain rate and lower rupture time. To cover all the four regions, strain rates from 10E−5/s to 10E−9/s are indicated in the figure.

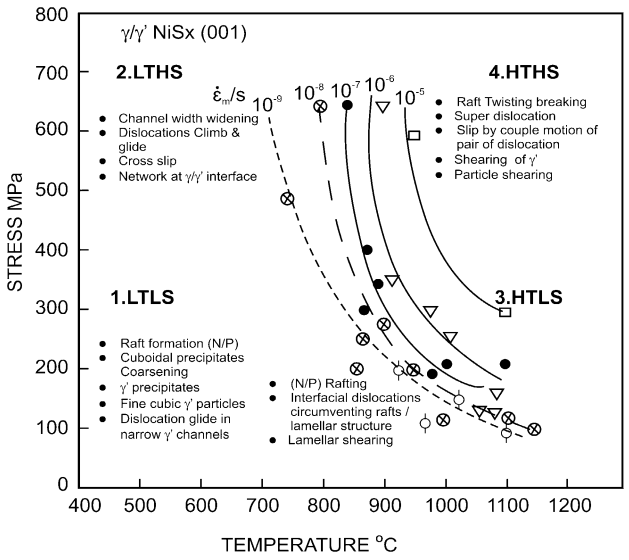

Fig. 9 Deformation mechanism map of first generation NiSX alloy

5.2 Classification and Identification of Regions and Mapping of Second Generation Alloys

5.2.1 Introduction

The factor that distinguishes the second generation from the first generation of the NiSX super alloys is the addition of the refractory element Rhenium, Re, around 4% generally. Addition of Re in the second generation alloys in the proper range has been found to be beneficial in reducing the deformation rate and increasing the creep rupture time by two or three fold.

5.2.2 Microstructural Regions in the Second Generation Alloys [15, 27, 28, 32, 35]: Microstructural Mechanisms and Deformation Mapping

The deformation mechanism map of second generation NiSX alloy is shown in Fig. 10. It can be divided into three regions as discussed below for the second generation of NiSX. It takes into account the role of Rhenium in microstructural changes in the three regions.

1. Low temperature region T < 800 °C (*no rafting, *gamma-prime particles and gamma matrix intact, *reduced diffusion, *increased misfit, *shearing of particle at high stress region, *matrix deformation at low stress region, dense dislocation tangles pile up at the interface of gamma prime)
2. Inter dendrite region 800 °C < T < 900 °C (*TCP formation, *inter dendrite, *high fraction of gamma prime, *low amount of refractory metals, *tendency for gamma prime to coarsen)

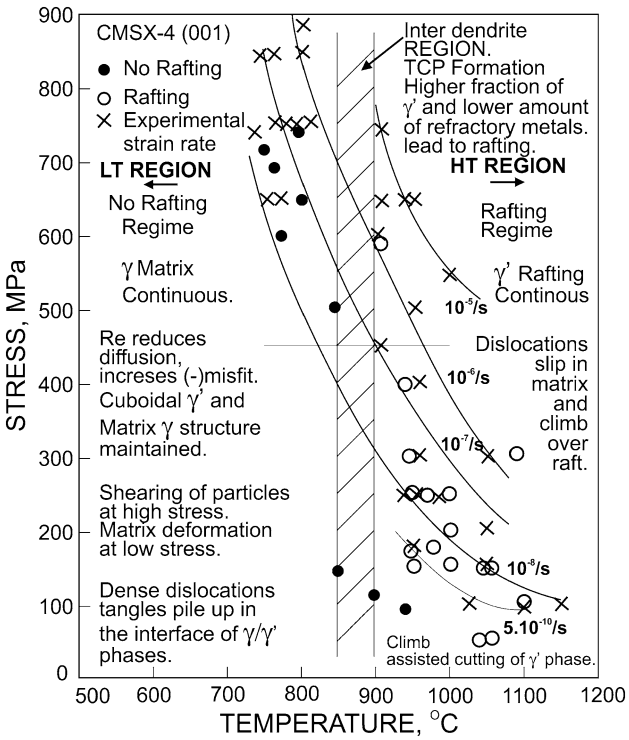

Fig. 10 Deformation mechanism map of second generation NiSX alloy

3. High temperature region T > 900 °C
(*coarsening of gamma prime precipitates, *raft formation, *dislocation slip in matrix and climb over raft, *climb associated cutting of gamma prime raft)

The inter dendrite region ID (2) separates the LT region (1), and the HT region (3).

In general, in the LT region the initial structure is kept in tact and no raft formation is observed. In the temperature region of 800–900 °C, precipitation of TCP phase takes place, the inter dendrite region contains high fraction of gamma prime phase and lower amount of refractory elements. Both these factors cause the I.D. region to initiate rafting. In the HT region, rafting and other dislocation activities control the deformation.

The mechanisms in these three regions are discussed below.

LT region, $T < 800\ ^{\circ}C$

In the LT region there is no formation of rafts. Rhenium reduces the diffusion. The cuboidal gamma prime precipitates and the horizontal and vertical gamma matrix channels are maintained and gamma matrix is continuous. In this region, the deformation is confined to the gamma matrix channel. The dislocations form cage structure around the precipitates. At high stress levels, shearing of precipitates takes place leading to super lattice stacking faults (SSFs). They are generated through particle shearing. After some creep deformation, larger number of stacking fault shearing events and, a high dislocation density exists in the matrix. Matrix deformation on {111} <110> is prevalent. Gamma prime/gamma interface is an important barrier to creep deformation.

Investigating the creep mechanism of CMSX-4, Schneider et al. [27, 28] found that the alloy that creep at 800 °C over a stress range of 650–925 MPa shows no raft formation and the high volume fraction of gamma precipitates remains cuboidal in all creep condition.

Inter dendrite (I.D.) region, $(T = 800-900\ ^{\circ}C)$

I D is the region which separates LT and HT regions.

In the 800–900 °C range, formation of thin platelets (in Re = 4–6% alloys) along the octahedral planes is observed. The gamma is essentially (Ni, Cr, W, Re), the gamma prime is basically (Ni, Cr)3 (Al, Ti, W) and the platelet precipitates (Ni, W) (Cr, Re) which is consistent with sigma formation. Formation of cellular colonies and secondary reaction zone (SRZ) are accompanied problems of rhenium addition leading to instability in microstructure.

The cellular colonies in the dendrite core are caused by large amount of Re segregation in this region. These cellular colonies in the dendrite core must be avoided and this can be achieved only by lowering the Re content and controlling the level of other refractory elements.

Different stages of microstructural changes in the ID region are a) changes from cuboidal to irregular facetted precipitates as temperature or time is increased specially in the region of T > 800 °C and b) nucleation of solid state dendrites leading to irregular precipitates and subsequent coarsening.

Re rejection from the growing gamma prime and its subsequent diffusion into the gamma matrix is observed at T ≥ 900 °C. Formation of high Re containing sigma phase limits the Re addition to the alloy. Limited Re addition can help in strengthening NiSX by solid solution means and by retarding gamma prime coarsening and reducing the deformation rate.

In the inter dendrite region, the precipitates are relatively free of dislocations. Dislocation activities take place in the horizontal and the vertical matrix channels. Shearing occasionally occurs by antiphase boundary (APB) mechanism.

HT region, $T = 900-1200\ ^{\circ}C$

In HTLS region with T > 950 °C and stress = 50–150 MPa, evolution of the gamma/gamma prime microstructure from cuboidal to plate like structure and well developed rafts and network of dislocations are observed. During coarsening and raft formation, rejection of Cr from the gamma prime and depletion of Ti in the gamma can be observed in front of the moving gamma–gamma prime interface.

At 950 °C/300 MPa, a directionally coarsened gamma/gamma prime structure prevails [13]. In the HT region of 950–1100 °C, it is found that gamma prime rafts that are formed are cut by dislocations. Climb-assisted cutting of gamma prime phase occurs in which vacancies are exchanged between the components of super partials. This mechanism appears to be a possible rate controlling step in creep of CMSX-4

In HT region (T > 900 °C) high density of dislocation activity in the gamma channels and the hexagonal cell structure of the interfacial net works take place. The cuboidal gamma prime phase is transformed into rafted structure. Dislocations slipping in the matrix and climbing over the raft or a few <110> super dislocations shearing into the rafted gamma prime phase are the dominant mechanism at relatively high temperature.

5.3 Comparison of Deformation Mechanisms and Maps of First and Second Generation of NiSX Alloys

From the deformation mechanisms discussed and the maps developed of the NiSX super alloys, as shown in Figs. 9 and 10, the following differences can be observed.

(a) There is coarsening of gamma prime precipitates leading to the formation of rafts in the low temperature regions in both LTLS and LTHS in the first generation alloys.

The microstructure with gamma prime particles and continuous gamma matrix channels is stable up to about 800 °C in the second generation alloys.

(b) Inter dendrite regions and changes that are conducive to the formation of TCP phases in the temperature range of 800–900 °C are observed in the second generation alloys.

This is absent in the first generation alloys.

(c) In the HT region, rafting, widening of gamma matrix channels are common in both generations of alloys. However, TCP appears to be dominant in the second generation alloys.

(d) There is a shift in the strain rate contours to the right in the second generation alloys as compared to the first generation alloys, indicating improved creep properties of the second generation NiSX due to Rhenium addition.

6 Conclusion

Based on the published research literature on the emerging turbine blade materials, first and second generation of NiSX, deformation mechanism maps with stress and temperature as coordinates have been constructed indicating the different regions, the dominant deformation mechanisms and the role of diffusion, dislocations, precipitation of gamma prime, and rafting that contribute to the change in microstructure. Constant strain rate contours are also shown in the maps. The maps can be further improved by incorporating contours of rupture time and other parameters useful to the alloy designers.

Acknowledgement The authors are grateful to Prof. B. Bhaskar Ramamurthi, Director, IIT Madras for his kind permission to publish this paper. We wish thank Dr. S. Madhavan for all his support in preparing the manuscript.

References

1. Biermann H, Tetzlah U, von Grossmann, and Mughrabi H, *Scr Mater* **43** (2000) 807.
2. Caron P, and Khan T, *Mater Sci Eng* **61** (1983) 173.
3. Chatterjee D, Hazari N, Das N, and Mithra R, *Mater Sci Eng A* **528** (2010) 604.
4. Cheng K Y, Jo C Y, Jin T, and Hu Z Q, *Mater Des* **31** (2010) 968.
5. Diologent F, and Caron P, *Mater Sci Eng A* **385** (2004) 245.
6. Fahrmann M, and Wolf J G, *Mater Sci Eng A* **210** (1996) 8.
7. Giamei A F, and Anton D L, *Metall Trans* **16A** (1985) 1997.
8. Grosdidier T, Hazotte A, and Simon A, *Mater Sci Eng A* **256** (1998) 183.
9. Safari J, and Nategh S, *Mater Sci Eng* A **499** (2009) 445.
10. Kamaraj M, Serin K, Kolbe M, and Eggeler G, *Mater Sci Eng A* **319** (2001) 796.
11. Kamaraj M, *Sadhana* **28** (2003) 115.
12. Kamaraj M, Mayr C, Kolbe M, and Eggeler G, *Scr Mater* **38** (1998) 589.
13. Lang C H, Schneider W, and Mughrabi H, *Acta Metall Mater* **43** (1995) 1751.
14. Luo Y S, Liu S Z, and Sun F L, *Mater Rev* **8** (2005) 55.
15. Maclachlan D W, and Knowles D M, *Metall Mater Trans A* **31A** (2000) 1401.
16. Masakazu Saito T, Aoyama K, and Hidaka H, *Tamaki Scr Mater* **34** (1996) 1189.
17. Veron M, Brechet Y, and Francois L, *Super Alloy* (1996) 181.
18. Nabarro F R N, and de Viliersv H L, *The Physics of Creep*, Taylor and Francis, London (1995).
19. Nabarro F R N, Cress C M, and Kotschy P, *Act Mater* **44** (1996) 3189.
20. Nathal M V, and Ebert L J, *Metall Trans A* **16A** (1985) 1849.
21. Nathal M V, and Ebert L J, *Metall Trans A* **16A** (1985) 427.
22. Nathal M V, *Metall Trans*. **18A** (1987) 1961.
23. Pamela H, Berglin L, and Jansson C *Scr Mater* **40** (1999) 229.
24. Pollock T M, and Argon A S. *Acta Metall Mater* **40** (1992) 1.
25. Pollock T M, and Argon A S. *Acta Metall Mater* **42** (1994) 1859.
26. McKay R A, and Ebert E J, *Metall Trans* **16A** (1985) 1969.
27. Schneider W, and Mughrabi H, *Proceedings of the 5th International Conference on Creep and Fracture of Engineering Materials and Structures* (eds: B. Wilshire and R.W. Evans) The Institute of Materials, London, 1993 209.
28. Schneider W, Hammer J, and Mughrabi H, *Super Alloys* (1992) 589.
29. Shi L, Yu J J, Cui C Y, and Sun X F *Mater Sci Eng A* **635** (2015) 50.
30. Tian S, Jiang C, Zhang S, Shang L, Shu D, and Xie J, *Mater Sci Eng* A **613** (2014) 184.
31. Sugui T, Su Y, Qian B J, Yu X F, Liang F S, and Li A N, *Mater Des* **37** (2012) 236.
32. Sugui T, Zeng Z, Fushun L, Zhang C, and Li C, *Mater Sci Eng A* **543** (2012) 104.
33. Tien J K, and Cobley S M, *Metall Trans* **2** (1971) 543.
34. Tian S, Zhang J H, Xu Y B, Hu Z Q, Yang H C, and Wu X, *Metall Trans A* **32** (2001) 2947.
35. Tian S, Wang M G, Yu H C, Yu X F, Li T, and Qian B J, *Mater Sci Eng A* **527** (2010) 4458.
36. Tinga T, Brekelmans W A M, and Geers M G D, *Comput Mater Sci* **47** (2009) 471.
37. Yuan Y, Kawagishi K, Koizumi Y, Kobayashi T, Yokokawa T, and Harada H, *Mater Sci Eng A* **608** (2014) 95.